inventions

MDPI

Article

Analysis of Thermo-Hygrometric Conditions of an Innovative Underwater Greenhouse

Giovanni Tanda [1,*], Samuele Memme [1], Gabriele Cucchia [2] and Sergio Gamberini [2]

[1] Dipartimento di Ingegneria Meccanica, Energetica, Gestionale e dei Trasporti (DIME), Università degli Studi di Genova, 16145 Genoa, Italy
[2] Mestel Safety Srl, Ocean Reef Group, 16010 Sant'Olcese (Genoa), Italy
* Correspondence: giovanni.tanda@unige.it

Abstract: Nemo's Garden® Project aims at creating a green, alternative, and original agriculture system based on underwater greenhouses (biospheres) developed for areas where plant growth is difficult in the terrestrial environment due to climate conditions and new global warming issues. Experiments were designed and performed to measure the thermal and hygrometric behaviour inside the biosphere; a simple theoretical model was developed to analyse the temperature and humidity of the air inside the biosphere in dynamic conditions and to interpret the experimental observations. The main findings of this research were: (i) the photosynthetically active radiation measured inside the underwater biosphere was 25–30% of that at sea level, (ii) the air temperature and relative humidity inside the biosphere showed cyclic daily variations that permitted a water evaporation/vapour condensation process, allowing the self-production of water for plant irrigation, and (iii) the results given by the lumped-parameter theoretical model were in a good agreement with the experiments.

Keywords: underwater greenhouse; air temperature; air relative humidity; photosynthetically active radiation; biosphere

check for updates

Citation: Tanda, G.; Memme, S.; Cucchia, G.; Gamberini, S. Analysis of Thermo-Hygrometric Conditions of an Innovative Underwater Greenhouse. *Inventions* **2022**, *7*, 118. https://doi.org/10.3390/inventions7040118

Academic Editor: Eugen Rusu

Received: 6 November 2022
Accepted: 5 December 2022
Published: 7 December 2022

1. Introduction

Underwater agriculture represents an alternative system for the growth of plants and vegetables; it is ecological as it does not require the use of pesticides and is self-sustainable due to the internal production of fresh water associated with seawater evaporation and internal condensation processes. Nemo's Garden® Project, promoted by the Ocean Reef Group, started in 2012 with the development of dome-shaped underwater greenhouses submerged in the northern Mediterranean Sea (Ligurian Sea, Italy). The purpose of this project, seemingly the first to investigate plant growth in an underwater environment, was to create alternative agricultural methods—ones specially dedicated to those areas where environmental conditions make plant growth extremely difficult, i.e., regions where both a lack of fresh water and fertile soils and extreme, hot temperature conditions occur.

Systematic studies on the influence of the marine environment on plants grown underwater have been carried out since 2015; several plant species (e.g., basil, red salad, beans) have been cultivated by sowing seeds in hydroponic or soil substrates [1,2]. This pioneering plant growth system may be applied to grow food and/or spice plants, as well as species of pharmaceutical interest, whose useful secondary metabolites may increment/change in a desirable direction due to the various stress conditions they are subjected to [2]. Analyses performed on basil growth underwater demonstrated that total chlorophyll, total carotenoids, and total polyphenols were present in higher amounts in the underwater greenhouses, with a 31% and 13% increase in antioxidant activity and polyphenol content with respect to the same plant coming from ground cultivation, with no differences in taste and appearance [2]. Despite further studies being needed to assess the adaptation of

distinct species to underwater conditions—especially the effects of increased pressure—these preliminary outcomes seemingly show superior properties in plants from underwater agriculture.

Due to its innovativeness and originality, a literature search did not uncover any prior publication dealing with this topic, except for the above-mentioned references involving some of the Ocean Reef Group staff. On the other hand, in recent years, the DIME Dept. of the University of Genoa, Italy has gained experience in the study of thermal systems in dynamic conditions (e.g., modelling of greenhouses as a function of greenhouse geometry and solar radiation characteristics [3,4] and experimental and theoretical analysis of thermal transients inside cabinets with electronic devices [5]). A fruitful collaboration between the Ocean Reef Group and the University of Genoa started in 2015 to provide an insight into the thermal and hygrometric conditions inside an underwater greenhouse.

The aim of this research is twofold: the experimental investigation of temperature and humidity transients inside underwater greenhouses and the theoretical modelling of the involved heat and mass transfer processes. The main features of underwater greenhouses are described in Section 2; the same Section provides descriptions of the measurements performed inside a representative greenhouse and a theoretical, lumped-parameter model, developed to interpret the physical mechanisms occurring inside the underwater greenhouse. The results are presented and discussed in Section 3, while the main findings of this investigation are summarized in Section 4.

2. Materials and Methods

2.1. The Underwater Greenhouse

Nemo's Garden® is located close to the coast of Noli (Liguria, Italy), 70 km from Genoa, Italy and consists of several underwater greenhouses anchored to the sea bottom at a 5-to-12 m depth and about 100 m from the shoreline. The characteristic structure of the Nemo's Garden® underwater greenhouse is illustrated in Figure 1; it consists of a transparent plastic dome (termed the "biosphere") to let sunlight reach the growing plants and an internal metallic frame used to anchor the structure to the seabed, to provide stability and to allow internal access to operators. As shown in the figure, a large bubble of air (pumped inside after the biosphere's installation) is trapped inside the hemispherical cavity created by the dome. The air trapped in the biosphere is confined, on the dome baseplate, by the open seawater (without any physical separation, e.g., a solid frame). Despite the solar radiation attenuation caused by the seawater layer, the interior of the biosphere undergoes a cyclic variation in air temperature over each day, with daily peaks significantly higher than the water temperature (which is rather stable over time on a daily basis). This effect, in concert with the solar radiation reaching the biosphere, contributes to plant growth in an environment with rather stable climatic conditions (unaffected by extreme weather phenomena that may occur above sea level) and free of external air contaminants (pollution, parasites, etc.). The sea water that evaporates from the water–air interface at the biosphere's bottom surface tends to condense on the inner surface of the dome, producing fresh water that is potentially useful for plant irrigation. In fact, the condensed water droplets drain by gravity from the dome's surface directly over the plants, which are located close to the inner surface in a spiral arrangement or over an annular shelf running along a sectional plane parallel to the water–air interface. A fan installed on the top of the interior dome's surface provides a uniformity of air temperature and relative humidity inside the biosphere.

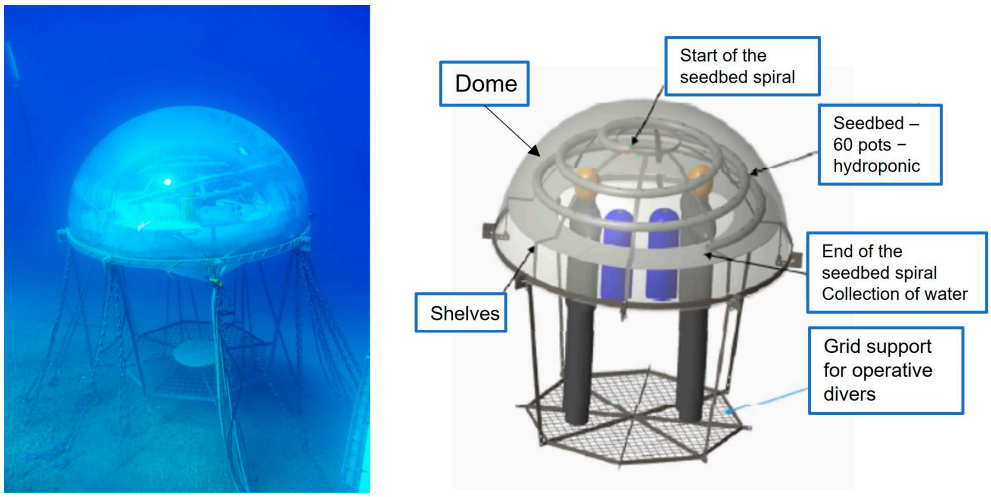

Figure 1. The underwater greenhouse (biosphere): in-situ photograph and description of its main elements.

Each biosphere is equipped with sensors for the continuous monitoring of environmental parameters—mainly air temperature, relative humidity, CO_2 and O_2 concentrations, and water temperature outside the biosphere. Webcams and intercom full duplex communication systems are also present in each biosphere to allow the continuous monitoring of plant growth and the communication of operators (when inside the biosphere for maintenance or plant collection) with the onshore lab. Some measurements gathered during the summertime of the year 2015 are reported in Figure 2, showing the air temperature, the water temperature, and the air relative humidity inside a biosphere. Typical daily air temperature excursions of about 3 °C from the minimum value reached overnight (and approximately equal to the water temperature) were recorded, together with daily air relative humidity variations of, typically, between 85 and 100%.

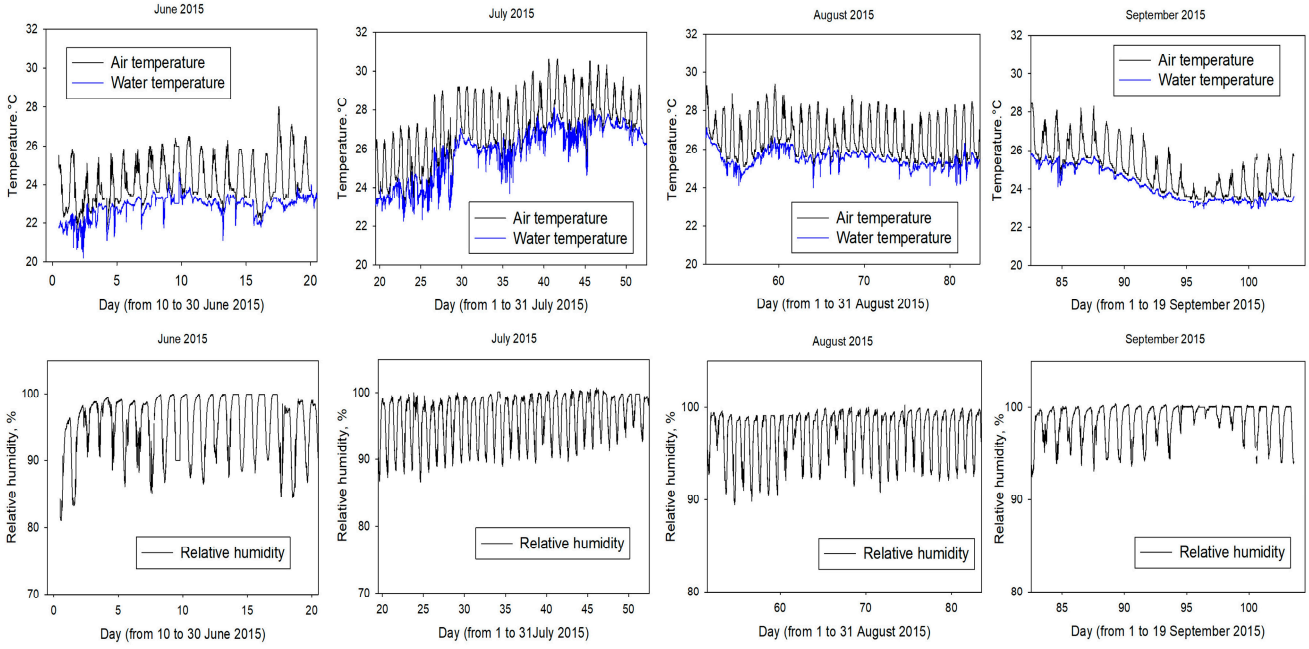

Figure 2. Measured variations over time of air and water temperature (**top**) and air relative humidity (**bottom**) during the summertime of the year 2015 in an underwater greenhouse.

Figure 3 displays a sequence of three pictures of a biosphere interior taken on three different days (with about a 20-day interval), showing the plant arrangement, their growing sequence, the fan at the dome top, and the seawater–air interface at the dome bottom.

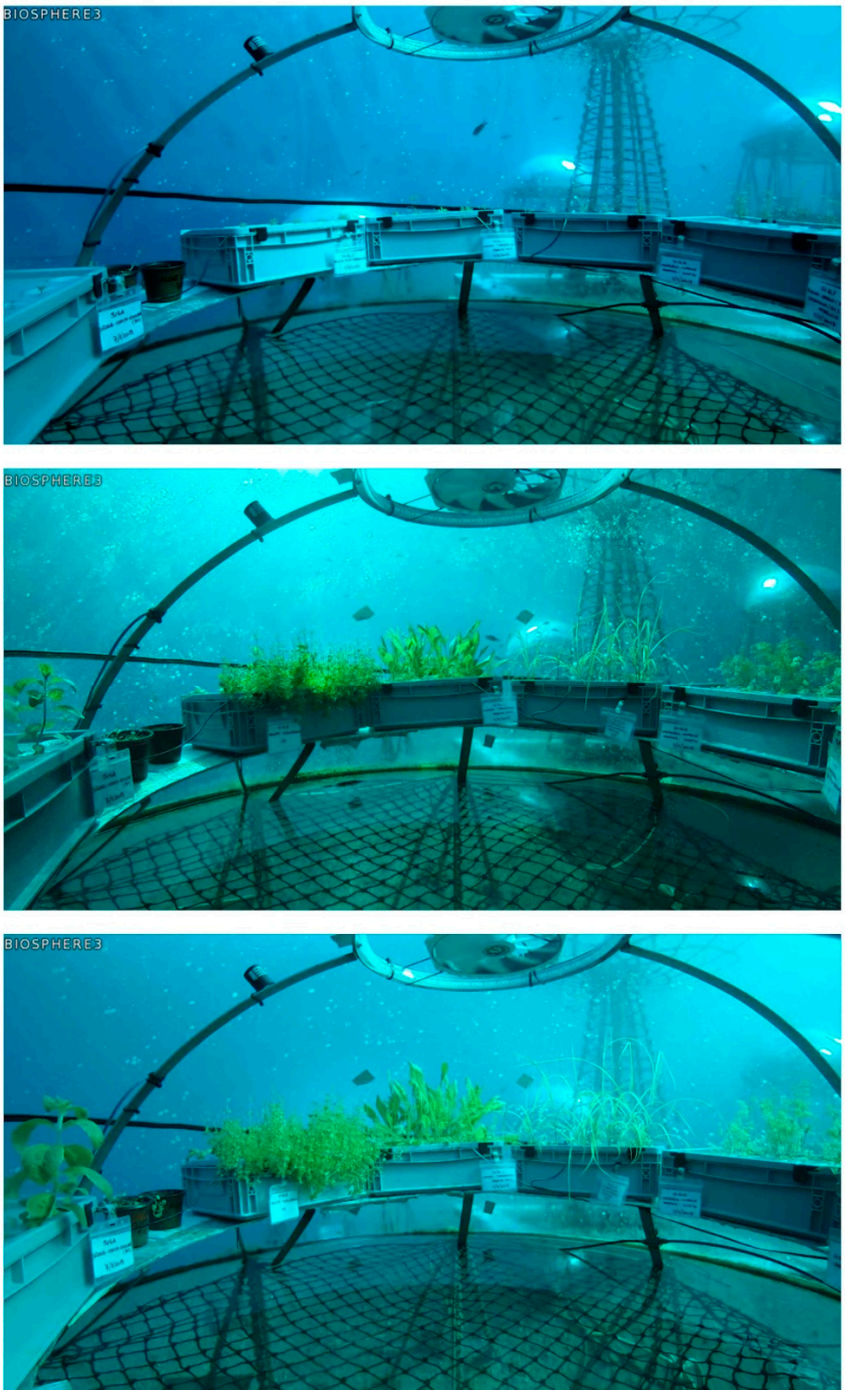

Figure 3. Photographic illustrations of a biosphere interior. From top to bottom: 12th day, 31st day, and 47th day after plant sowing.

2.2. The Experiment

An experiment was designed to investigate, in detail, the thermal and hygrometric conditions inside a representative biosphere. In particular, the experimental investigation was concerned with the following measurements (basically involving a large number of sensors with respect to those typically installed in the Nemo's Garden® biospheres):

- the internal air temperature of the biosphere,
- the water temperature outside the biosphere and immediately below the air–water interface at different depths,
- the inner-surface temperature of the transparent biosphere dome,
- the internal air relative humidity,
- the solar radiation in the PAR (Photosynthetically Active Radiation) wavelength range at sea level and inside the biosphere. As is known, PAR encompasses the solar irradiance only in a fraction of the wavelength solar spectrum, and it is this that plants are able to use in the process of photosynthesis.

The experimental measurement campaign was performed in July 2019 inside a biosphere with a diameter of 2 m, fixed at a depth 8 m under sea level. Plants were not present in the biosphere during experiments to avoid any interacting effects (if any) on the thermal and hygrometric behaviour. During the period of observation, local weather in Noli (Liguria, Italy) was characterised by daily-average air temperatures varying from 18 °C (on 15 July) to 32 °C (on 24 July), with sunny days prevailing (25 out of 31 days); the average values in this period for the daily mean, minimum, and maximum air temperature were 27.2, 22.4, and 29.5 °C, respectively.

The water and air temperatures were measured using waterproof temperature sensors DS18B20 (Dallas semiconductor inc.), calibrated to ±0.1 °C, positioned inside the biosphere at the water–air interface and immediately below it, and in the seawater outside the biosphere at the same depth. The air temperature sensor, located in approximately the centre of the biosphere, was shielded to prevent direct solar irradiation.

An infrared thermometer (Raytek MI3), calibrated to ±0.3 °C and positioned at a 10 cm distance from the internal surface of the dome, was employed to detect the surface temperature of the biosphere dome. The air's relative humidity was measured using an integrated temperature/humidity sensor (AM2315, Aosong) calibrated to ±1% (*Rh* units), using six points of different humidity in the 10–98% range, and a chilled mirror (Michell Instrument Optidew model) as a reference device.

The measurement of light intensity for photosynthetic use is a fundamental aspect to understand what happens to plants and to establish whether there are controllable actions through engineering means to optimize growth, control the spread of diseases, and establish a link between the organoleptic qualities of biomass and growth conditions. The attenuation of light in water depends on the angle of incidence of the radiation relative to the free surface, the rippling of the waves, the water transparency, the diffuse and direct fractions of solar radiation, the depth of the water, and the prevailing wavelength of the light wave (sunrise, noon, sunset). Very little scientific information is available on PAR water attenuation; for this reason, a measurement of PAR outside and inside the water was deemed to be fundamental to this study. Solar radiation in the 400–700 nm range was measured through two LP PAR 01 sensors (DeltaOhm)—one located at sea level (onshore lab) and the other inside the underwater biosphere. The outputs of the two sensors were checked against each other in an external environment and their agreement was within the declared uncertainty (6%) limits of the devices.

Figure 4 schematically shows the locations of the sensors inside and outside the biosphere; all measurement devices were connected to an Arduino controller and data were automatically acquired every five minutes—except for the external PAR device, whose signal was detected every 30 min.

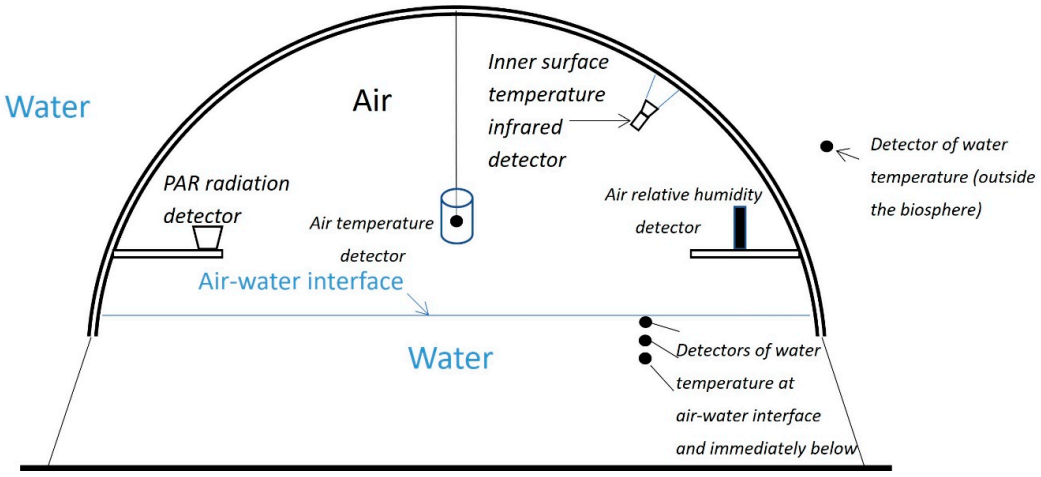

Figure 4. Location of the sensors employed in the experiment.

2.3. The Theoretical Model

A lumped-parameter model was developed to analyse the dynamic thermal and hygrometric behaviour of the underwater biosphere and to provide a possible interpretation of the observed physical phenomenon. The description of this model is facilitated by reference to Figure 5: the biosphere, located at a depth under sea level denoted by z, contains air at the temperature T_a and objects at the temperature T_b. The air is surrounded by the transparent dome at temperature T_d, and seawater at temperature T_w. Solar irradiance (G_0 at the sea level) is attenuated as it travels along the seawater layer by a factor given by $\exp(-z\,K_D)$, where K_D is an attenuation coefficient; i.e., the solar radiation entering the biosphere G_z is calculated as $G_z = G_0\, e^{-zK_D}$. This model assumes both heat and mass transfer at the water/air interface, controlled by a heat transfer coefficient h and a mass transfer coefficient h_m, deduced by exploiting the heat/mass transfer analogy and expressed as $h_m = h\, Le^{-0.67}/(\rho_a c_a)$—where Le is the Lewis number, while ρ_a and c_a are the density and specific heat of the air [6].

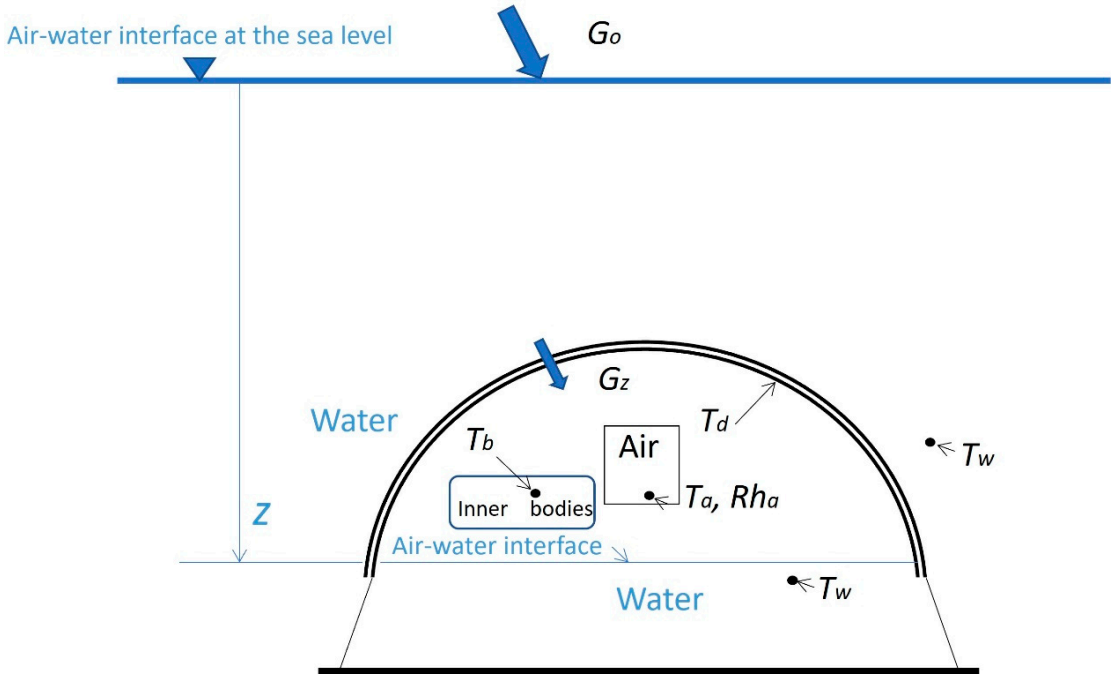

Figure 5. Schematic drawing of the biosphere and the variables included in the model.

The governing equations for the temperature of the air T_a and the inner objects T_b and for the air relative humidity Rh_a are:

$$dT_a/dt = [h\ A_b\ (T_b - T_a) + h\ A_w\ (T_w - T_a)]/(m_a\ c_a) \quad (1)$$

$$dT_b/dt = [h\ A_b\ (T_a - T_b) + \alpha_b\ A_b\ G_0\ \exp(-z\ K_D) + \sigma\ \varepsilon_b\ A_b({T_d}^4 - {T_b}^4)]/(m_b\ c_b) \quad (2)$$

$$dRh_a/dt\ =\ \left(\dot{m}_{evap} - \dot{m}_{cond}\right)/m_{v,sat} \quad (3)$$

In the above equations, A is the heat transfer area, α_b and ε_b are the solar radiation absorption coefficient and the emissivity of the inner objects, σ is the Stefan–Boltzmann constant, $m_{v,sat}$ is the mass of the saturated vapour at the air temperature T_a, and the subscripts a, b, d, and w refer to the air, inner objects, dome, and water, respectively. Due to the presence of the long-wavelength radiation heat transfer between the inner objects (assumed as a convex-shaped diffuse-gray body inside a cavity) and the inner surface of the dome, all temperatures must be expressed in [K]. The evaporation and condensation mass flow rates $\dot{m}_{evap}$ and $\dot{m}_{cond}$ are given by:

$$\dot{m}_{evap}\ =\ h_m\ A_\omega\ \left(\rho_{v,sat!} - Rh_a\ \rho_{v,sat}\right)\ F_{evap} \quad (4)$$

$$\dot{m}_{cond}\ =\ h_m\ A_d\ \left(\rho_{v,satd} - Rh_a\ \rho_{v,sat}\right)\ F_{cond} \quad (5)$$

where the mass transfer coefficient h_m is taken to be equal for both the evaporation and condensation processes and ρ_v represents the water vapour density, with the subscripts *sat*, *satw*, and *satd* denoting its evaluation at the air, water, and dome temperature, respectively.

The function F_{evap} equals 1 when the calculated Rh_a falls in the range 0–1; otherwise, it is set to 0 (no evaporation). The function F_{cond} equals 1 when the calculated Rh_a falls in the range 0–1 and the dome temperature T_d is lower than the dew-point temperature (depending in turn on T_a and Rh_a); otherwise, it is 0 (no condensation). For the sake of simplicity, no equations are written for T_w and T_d—both considered as constant, known, and equal to each other.

Provided that the heat/mass transfer surface areas, heat/mass transfer coefficients, mass of the inner objects, physical properties, seawater temperature, and solar radiation at the sea level (and its variation over time) are regarded as the input data of the problem, the solution of the set of equations for the unknown variables T_a, T_b, Rh_a, $\dot{m}_{evap}$, and $\dot{m}_{cond}$ allows for the prediction of the thermal and hygrometric dynamic behaviour of the biosphere.

3. Results and Discussion

A presentation of the experimental measurements is given for two representative consecutive days—namely, 13 and 14 July 2019. The weather was sunny on the first day (external air temperature between 23 and 32 °C) and sunny with some light cloud at times on the second day (external air temperature between 22 and 29 °C).

As reported in Figure 6, where the external and internal PAR are displayed, the light absorption of the seawater layer in the 400–700 nm range was noticeable, and only a fraction between 25 and 30% of the PAR recorded outside was able to reach the biosphere. Despite light attenuation being sensitive to the wavelength—with blue light (450 nm) less strongly absorbed than red light (650 nm) [7]—as the entire PAR range was taken into consideration, the recorded percentage level of attenuation was consistent with [8], who experimentally found an attenuation coefficient of 0.15 m^{-1}, which corresponds to a PAR—at an 8 m depth—equal to 30% of the PAR at sea level, in line with the observed values.

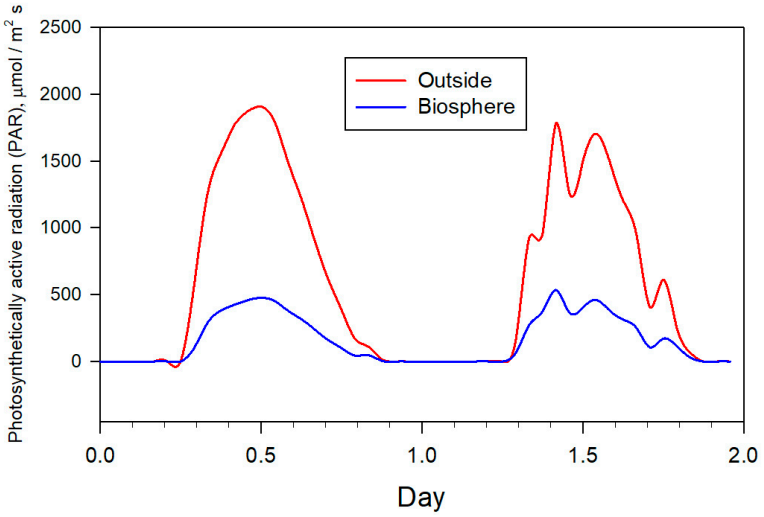

Figure 6. Measured PAR at sea level and the underwater biosphere level.

The corresponding air, surface, and water temperatures registered over the same periods are plotted in Figure 7. Despite the marked attenuation, the radiation penetrating the biosphere and that absorbed by the internal objects induced an air temperature increase, from the nocturnal level, of up to 4.7 °C during the first day of observation and 4.2 °C during the second day. In addition to the air temperature changes over time, Figure 7 shows the interior surface temperature of the biosphere dome recorded by the infrared (IR) sensor and the water temperatures evaluated in the vicinity of the water–air interface and in the seawater outside the biosphere (as indicated in the sketch of Figure 4). The inner surface temperature of the dome exhibited the same trend as the air temperature, with a damping effect exerted by the thermal inertia of the 2 cm-thick Plexiglas wall; it exceeded by about 1 °C the water temperature during the night and by up to 1.5 °C when solar radiation was present. Conversely, the seawater temperature was rather stable over each day (having only long-term variations, as inferred from Figure 2), with daily excursions of less than ± 0.5 °C around the mean value. The water layer in contact with the air bubble trapped inside the biosphere was slightly heated at the interface, but 1 cm below exhibited the same temperature as the seawater outside the biosphere measured at the same depth under sea level.

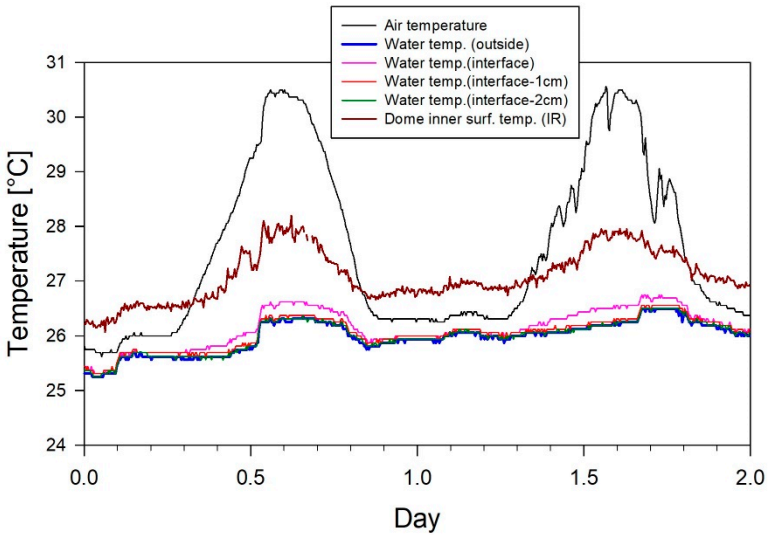

Figure 7. Measured air, inner surface, and water temperature inside the underwater biosphere.

The cyclic air temperature increase documented in Figure 7 was reflected by a synchronous reduction in the internal air relative humidity, displayed in Figure 8 for the same two days of observation. Inspection of the figure shows that the relative minima of the relative humidity were concentrated during the maximum insolation, with the achievement of saturation conditions during the night. This cycling process, summarized in Figures 7 and 8, was deemed to ensure comfortable thermal and hygrometric conditions for plants, together with the sufficient levels of incoming radiation shown in Figure 6.

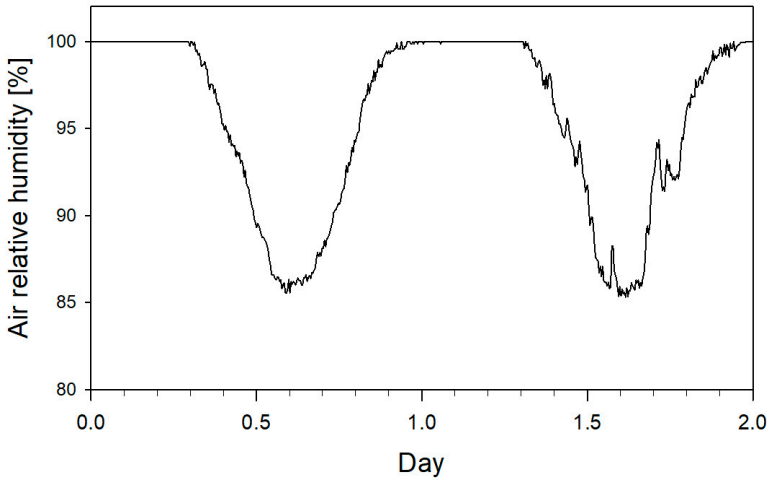

Figure 8. Measured air relative humidity inside the underwater biosphere.

The observed thermal and hygrometric conditions permitted the evaporation of seawater from the water–air interface at the bottom side of the biosphere, due to the favourable partial vapour pressure gradient during the warmer hours of the day. Since the temperature of the dome inner surface—affected by the relatively low temperature of the seawater surrounding the dome—was lower than the dew-point temperature for most of the day, the produced water vapour tended to condense over the inner surface of the dome itself, furnishing self-produced water for irrigation purposes.

In the original conceiving of the biosphere, the condensed water—serving as a fresh water irrigation source—drained by gravity directly onto the plants, providing their sustenance and growth. The collection and consequent re-use of the condensed vapour within the biosphere can be improved by using a radiator condenser with a fan. In this case, the coolant (the seawater that is spilled at a lower level than the biosphere and pumped into the circuit) flowing inside the radiator, removes the heat necessary for the condensation of the water vapour present in the air. Furthermore, there is the possibility of using a controlled Peltier module, i.e., relating the operating parameters of the Peltier element to the quantity of condensing flow. The control and stability of the Peltier temperature require a particular electronic circuit that adjusts voltage and current through an appropriate TEC (Thermo-Electric Cooler, or Peltier Cooler) controller and a temperature sensor; at the same time, the temperature of the cold surface is kept under control. The Peltier cold surface has been conceived for a future method based on a mini heat exchanger fed by cold water, as circulated from deeper sea layers with respect to the greenhouse location.

Figure 9 shows a comparison between the experimental measurements and the calculated results, in terms of the air temperature and relative humidity inside the biosphere, given by the model described by Equations (1)–(5). The input data for the calculations were consistent with the geometry and operating conditions of the investigated biosphere; more precisely, $T_w = T_d = 26$ °C (299.15 K), $m_a = 4.4$ kg, $m_b = 20$ kg, $h = 10$ W/m^{2}K, $Le = 0.86$, $\alpha_b = \varepsilon_b = 0.8$, c_a =1005 J/kg K, $c_b = 900$ J/kg K, $A_b = 1$ m^2, $A_w = 3.14$ m^2, and $A_d = 6.28$ m^2, while the initial air and body temperatures were set at 26 °C (299.15 K) and the initial air relative humidity at 100%. The hourly solar irradiance at sea level, for the days of observation, was taken from a local weather station and attenuated by the factor $\exp(-z\,K_D)$, with

z = 8 m and K_D = 0.15 m^{-1}. An inspection of Figure 9 reveals that the theoretical model captured with a satisfactory level of confidence the thermal and hygrometric behaviour of the biosphere. As a possible, important interpretation—provided by the model—of the experimentally observed mechanism of cyclic heating of the air in the biosphere (confirmed by the calculations), it is worth noting that—according to Equation (2)—the objects inside the biosphere receive and accumulate low-wavelength radiant heat that is transferred by convection and high-wavelength radiation to the air and to the interior side of the dome, thus promoting the air temperature increases during the sunny hours of the day; when the solar radiation vanishes, the calculated air temperature rapidly approaches that of the seawater. In fact, without any solar radiation absorption from the objects inside the biosphere (i.e., setting α_b = 0), the calculated air and water temperature coincide, as the incoming solar radiation is expected to pass through the biosphere without affecting the thermal balance of the internal air. Furthermore, since the model was based on a simple lumped-parameter analysis, it could be easily implemented to consider the presence of devices (radiator condenser, Peltier cooler) capable of increasing the amount of condensed water vapour inside the biosphere.

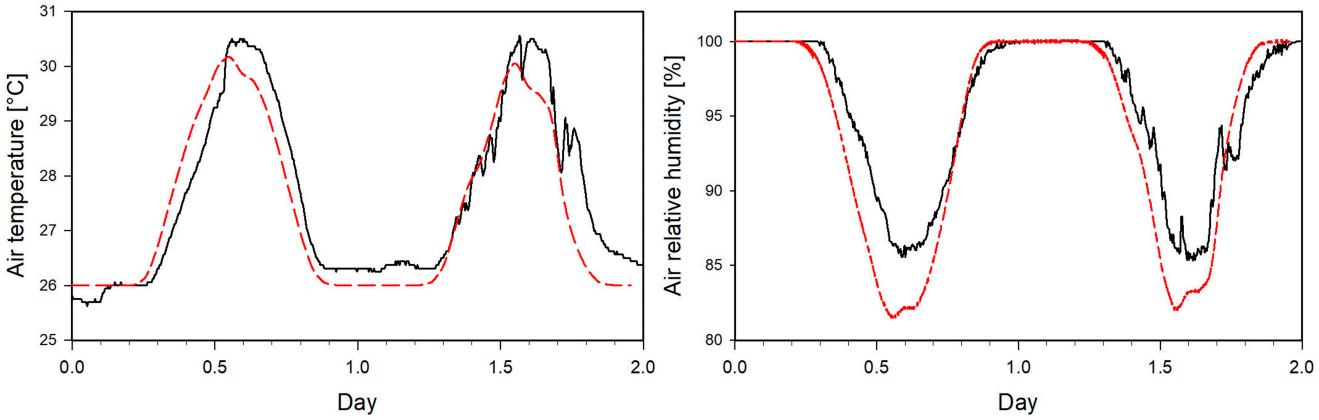

Figure 9. Measured (solid lines) and calculated (dashed lines) air temperature and relative humidity inside the underwater biosphere.

4. Conclusions

In this study, the thermal and hygrometric conditions inside an underwater greenhouse used for alternative and sustainable agriculture were experimentally and theoretically investigated. One of these greenhouses (called biospheres) belonging to the so-called Nemo's Garden® was instrumented to obtain precise indications on the temporal evolution of the most significant factors, i.e., the water and air temperature, relative air humidity, and photosynthetically active radiation (PAR), at the surface and in the biosphere. The experimental data were used for the validation of an interpretative, lumped-parameter model of the phenomenon.

The most significant results are as follows:

- the measured attenuation of PAR at a 8 m depth, reduced to 25–30% of that present at the surface—consistent with the literature data—was nevertheless found to be sufficient for plant growth and life, such that it induced significant warming of the air in the biosphere;
- the temperature and relative humidity of the air in the biosphere showed daily fluctuations that were offset from each other (the humidity was lowest when the temperature was highest): this behaviour permitted the evaporation of seawater during the warmer hours of the day and vapour condensation over the inner surface of the dome when the temperature was below the dew point—thus providing water self-production for plant irrigation;

- the lumped-parameter model, which uses solar radiation at the surface and water temperature at depth as input data—along with the heat capacity of objects within the biosphere—provided calculated temperature and humidity variations over time in line with the experimental results and an interpretation of the observed cyclic thermo-hygrometric behaviour.

Author Contributions: Conceptualization, methodology, and writing: all authors; Conceiving and designing of Nemo's Garden: S.G. and G.C.; Designing of experiments and modelling: G.T. and S.M. All authors have read and agreed to the published version of the manuscript.

Funding: This research received no external funding.

Data Availability Statement: Not applicable.

Conflicts of Interest: The authors declare no conflict of interest.

References

1. Dini, G.; Princi, E.; Gamberini, S.; Gamberini, L. Nemo's Garden: Growing plants underwater. In Proceedings of the OCEANS 2016 MTS/IEEE Monterey 2016, Monterey, CA, USA, 19–23 September 2016; pp. 1–6. [CrossRef]
2. Pistelli, L.; Ascrizzi, R.; Giuliani, C.; Cervelli, C.; Ruffoni, B.; Princi, E.; Fontanesi, G.; Flamini, G.; Pistelli, L. Growing basil in the underwater biospheres of Nemo's Garden®: Phytochemical, physiological and micromorphological analyses. *Sci. Hortic.* **2020**, *259*, 108851. [CrossRef]
3. Ouazzani Chahidi, L.; Fossa, M.; Priarone, A.; Mechaqrane, A. Energy saving strategies in sustainable greenhouse cultivation in the mediterranean climate—A case study. *Appl. Energy* **2021**, *282*, 116156. [CrossRef]
4. Boccalatte, A.; Fossa, M.; Sacile, R. Modeling, design and construction of a zero-energy PV greenhouse for applications in mediterranean climates. *Therm. Sci. Eng. Prog.* **2021**, *25*, 101046. [CrossRef]
5. Tanda, G. Cooling solutions for an electronic equipment box operating on UAV systems under transient conditions. *Int. J. Therm. Sci.* **2020**, *152*, 106286. [CrossRef]
6. Bejan, A. *Heat Transfer*; J. Wiley & Sons, Inc.: New York, NY, USA, 1993.
7. Kettle, H.; Merchant, C.J. Modeling ocean primary production: Sensitivity to spectral resolution of attenuation and absorption of light. *Prog. Oceanogr.* **2008**, *78*, 135–146. [CrossRef]
8. Gómez, I.; Huovinen, P. Lack of physiological depth patterns in conspecifics of endemic Antarctic brown algae: A trade-off between UV stress tolerance and shade adaptation? *PLoS ONE* **2015**, *10*, e0134440. [CrossRef] [PubMed]